Chaos, Solitons & Fractals 44 (2011) 248–259

Contents lists available at ScienceDirect

Chaos, Solitons & Fractals

Nonlinear Science, and Nonequilibrium and Complex Phenomena

journal homepage: www.elsevier.com/locate/chaos

Border collision bifurcation curves and their classification in a family of 1D discontinuous maps

Laura Gardini [a], Fabio Tramontana [b,*]

[a] Università degli Studi di Urbino, Department of Economics, Society and Politics, Via Saffi 42, 61029 Urbino, Italy
[b] Università degli Studi di Pavia, Department of Economics and Quantitative Methods, Via S.Felice 5, 27100 Pavia, Italy

ARTICLE INFO

Article history:
Received 19 December 2010
Accepted 6 February 2011
Available online 12 March 2011

ABSTRACT

In this paper we consider a one-dimensional piecewise linear discontinuous map in canonical form, which may be used in several physical and engineering applications as well as to model some simple financial markets. We classify three different kinds of possible dynamic behaviors associated with the stable cycles. One regime (i) is the same existing in the continuous case and it is characterized by periodicity regions following the *period increment* by 1 rule. The second one (ii) is the regime characterized by periodicity regions of *period increment* higher than 1 (we shall see examples with 2 and 3), and by bistability. The third one (iii) is characterized by infinitely many periodicity regions of stable cycles, which follow the *period adding* structure, and multistability cannot exist. The analytical equations of the border collision bifurcation curves bounding the regions of existence of stable cycles are determined by using a new approach.

1. Introduction

A significant amount of research works have been recently published regarding piecewise smooth and piecewise linear systems because of their wide use in applications. Several models in engineering and physical sciences are of this kind (see [4–7,12,13,15,18–20,22,23,31,37,42]), as well as in economics (see [35,36]).

The first results on piecewise smooth systems date back to several years ago, for continuous models as well as for discontinuous systems ([24,25,30]). The main point in the analysis of non-smooth one-dimensional systems (continuous and discontinuous) is the occurrence of *border collision bifurcations* (BCB henceforth). The term was introduced by Nusse and Yorke in 1992 [32] (see also [33,34]), and now it is widely used. A cycle undergoes a BCB when a periodic point of the cycle collides with the point in which the system changes definition. BCBs can be responsible for example of the direct transition from a stable fixed point to a cycle of any period, to chaotic dynamics or to divergence.

Piecewise smooth systems can be classified in two types with different properties, although both characterized by BCB, that is: *continuous* models and *discontinuous* ones. The bifurcation properties of these two classes of maps are in fact quite different. For example, the BCBs occurring in the one-dimensional continuous unimodal piecewise-linear map in canonical form,[1] which can be used for the analysis of any other BCB occurring in continuous piecewise smooth maps, have been completely studied. The results can be found in some papers [26–28,32,34], see also [38] for a review. While regarding discontinuous one-dimensional maps, also piecewise-linear, only partial results exist. Several properties have been described (see [4,6,7]), but still the knowledge is far from a complete classification of all the possible dynamics. As recalled above, the researches associated with discontinuous maps started several years ago, with works by Leonov at the end of the 50th [24,25]. Recent results have been obtained in [21,8] and the technique there described, associated with two

* Corresponding author.
E-mail addresses: laura.gardini@uniurb.it (L. Gardini), fabio.tramontana@unipv.it, f.tramontana@univpm.it (F. Tramontana).

[1] The so-called skew-tent map.

0960-0779/$ - see front matter © 2011 Elsevier Ltd. All rights reserved.
doi:10.1016/j.chaos.2011.02.001

linear increasing branches, will be used also here, applied to the case of a piecewise linear discontinuous map with increasing and decreasing branches.

In this work we are interested in a piecewise linear discontinuous map in canonical form, giving results and equations for the generic cases. This kind of models are also used to describe some simple financial relations between chartists and fundamentalists, as those recently called of "bull and bear dynamics" [39,40]. From the seminal papers by Day [16,17], such simple models are up to date to interpret the financial crises. In particular the map in canonical form is used in [41], where we have analyzed some special cases associated with linear pieces having both positive slopes or both negative slopes. Other cases, associated with two positive slopes, have been investigated in [21]. Here we shall focalize the analysis to the case which is left to investigate, that is: one increasing and one decreasing branch, in which an equilibrium point always exists (stable or unstable). A feedback mechanism exists, so that the trajectories can never diverge, and the asymptotic dynamics are either periodic, or quasiperiodic, or aperiodic in some bounded cyclic chaotic intervals.

Our map includes as particular examples those considered in the recent literature (for example in [4,6,7]). As we shall see from the analysis of the general case, the possible dynamic occurrences are richer than those observed in the cited papers. In particular, we shall introduce the distinction between three different regimes with qualitatively different dynamic behaviors. In fact, we shall see that the case of a continuous map separates two different situations. In one only particular cycles may be stable, called principal (or maximal) cycles, whose periods follow the increment rule by 1 unit and bistability cannot occur. In the second one similar dynamics also occur, but besides the periodicity regions of these cycles, there are also regions with two different kinds of stable periodic orbits in families which follow the period increment by units higher than 1, associated with *overlapped periodicity regions, leading to bistability* (i.e. coexistence of two different attracting cycles, with periods differing by a constant). A third region will be classified (via the homoclinic bifurcation of the fixed point), associated with the existence of infinitely many periodicity regions, following the *period adding structure typical of the Farey rule*, i.e. between two existing periodicity regions associated with cycles of periods k_1 and k_2, also another periodicity region associated with a cycle of period $p = k_1 + k_2$ exists, and *no coexistence of cycles can occur*. It is in this period adding structure that we can use a quite new technique to determine the bifurcation curves analytically. This technique comes from an idea introduced by Leonov several years ago [24,25], in the case of increasing/increasing branches, recently improved in [21] and extended in [8]. Here it will be applied to different maximal cycles in the increasing/decreasing case. We are mainly interested in the families of stable cycles, and we shall see an iterative process to calculate families of related BCB curves.

The plan of the work is as follows. In Section 2 we introduce the map, a linear increasing branch in the left side (L) of the discontinuity point and a linear decreasing one in the right side (R), describing some of its properties, among which the degeneracy of all the flip bifurcations of any cycle, and the classification of the three cases (i), (ii) and (iii). In Section 3 we determine the BCB curves associated with the periodicity regions of cycles occurring in the region (i), having the symbolic sequence L^kR, and the related curves at which their degenerate flip bifurcation occurs. In Section 4 we consider the BCB curves associated with the periodicity regions of cycles occurring in the region (ii) which are overlapped in pair, and thus with bistability, illustrating a particular property in which three bifurcation curves intersect (two BCB curves and one degenerate flip bifurcation curve). In Section 5 we illustrate the properties of region (iii) where infinitely many periodicity regions exist associated with particular kinds of adding structure, different from the one presented in [21] but with the same dynamic properties. Section 6 concludes.

2. The map

The family of maps that we consider is given by

$$x' = T(x) = \begin{cases} f_L(x) = s_L x + m_L & \text{if } x < 0, \\ f_R(x) = s_R x + m_R & \text{if } x > 0, \end{cases} \tag{1}$$

where the parameters satisfy the following restrictions:

$$s_R < 0 < s_L < 1, \quad m_{L,R} > 0, \tag{2}$$

where $m_L \gtreqless m_R$, so that we have an increasing straight line for $x < 0$ and a decreasing branch for $x > 0$. The shape of the map (1) is shown in Fig. 1(a) and (b). However, the results and properties determined in the cases here considered, represented by the constraints in (2), also work when the shape of the map is as shown in Fig. 1(c) and (d) due to the symmetry property of the map $T(x)$:

$$T(x, s_R, s_L, m_L, m_R) = -T(-x, s_L, s_R, -m_R, -m_L). \tag{3}$$

As we limit the branch on the left to a slope positive and less than one, we have no equilibrium on the left side,[2] and the iterated points are pushed on the right side, where a negative slope exists, and in case of unstable fixed point, necessarily the generic trajectory is forced to return (after a finite number of iterations around the unstable fixed point) on the left side, where an increasing sequence will start again. Thus, the dynamics are in a natural way always bounded: they can never diverge. It is interesting to investigate the relevant regimes which can occur in this situation, specially when the fixed point on the right side, $x_R^* = \frac{m_R}{1-s_R}$, is unstable.

From Fig. 1(a) and (b) we can see the different situations which may occur:

(i) either the left branch ends above the right one, $f_L(0) \geqslant f_R(0)$, i.e. $m_L \geqslant m_R$, (as in Fig. 1(a)), and the map is continuous in the case of $m_L = m_R$, discontinuous otherwise;
(ii) or the left branch ends below the right one and above the fixed point $x_R^* \leqslant f_L(0) < f_R(0)$, i.e. $x_R^* \leqslant m_L < m_R$ (as in Fig. 1(b));
(iii) or the left branch ends below the fixed point, $0 < f_L(0) < x_R^*$ ($< f_R(0)$), i.e. $0 < m_L < x_R^*$ ($< m_R$).

[2] As $m_L > 0$ by assumption.

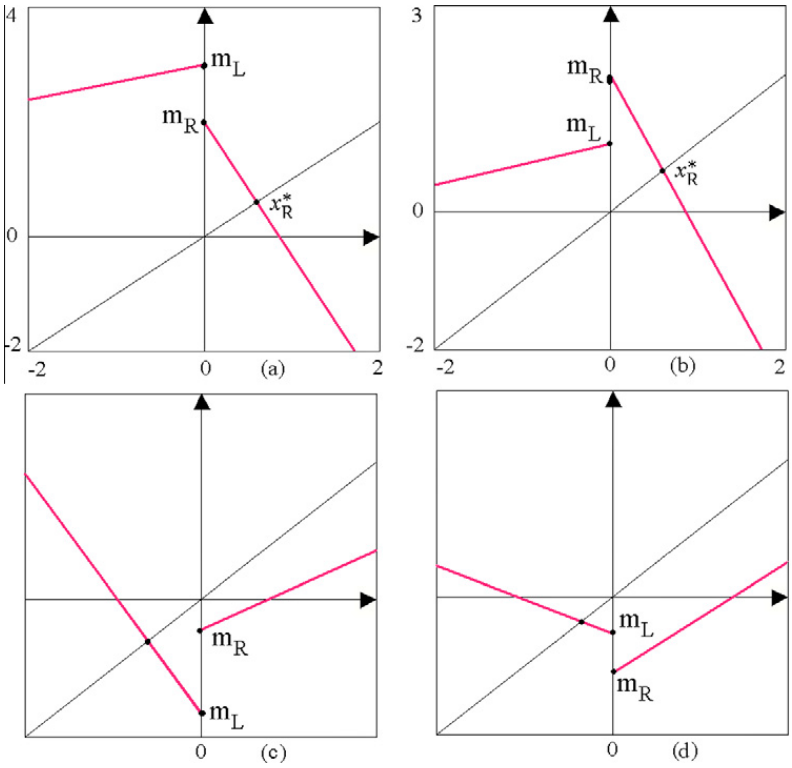

Fig. 1. Graph of the map at $s_R = -2.3$, $s_L = 0.3$, $m_R = 2$. In (a) $m_L = 3$. In (b) $m_L = 1$. The conjugate cases in (c) and (d).

The transition between the cases (ii) and (iii) is determined by the homoclinic bifurcation of the fixed point x_R^*. In fact, it is immediate to see that x_R^* is homoclinic in regime (ii) (also called a snap back repeller), and in that regime chaotic dynamics can exist. While no homoclinic point of x_R^* can exist in regime (iii). As we shall see, the main property existing in regime (iii) is the transition to regular dynamics, characterized by the non existence of chaotic dynamics.

As our results are generic and depend on all the parameters of the model, the equations giving the BCB curves and the degenerate flip bifurcations curves of the cycles occurring in the continuous case are the same as those detected for the discontinuous case in (i) with the particular choice of parameters $m_L = m_R$. However, we notice that the bifurcation structures in the chaotic regimes (with cyclical chaotic intervals) in discontinuous and continuous maps are different (and not investigated in this work).

Due to the linearity it is very easy to get the eigenvalue associated with some cycle. A periodic orbit having period $k = p + q$ with p points in the L side and q points in the R side, necessarily has eigenvalue $\lambda = s_L^p s_R^q$. Moreover, we shall see that in the case (i) defined above, all the stable cycles which may exist necessarily have negative eigenvalue, so that they can have only a bifurcation with eigenvalue $\lambda = -1$, which in our piecewise linear map is always degenerate. A degenerate flip bifurcation of a k-cycle is such that at the bifurcation value (when the eigenvalue is equal to -1), the map possesses an interval filled with $2k$-cycles (with the k-cycle in between) (see [38]). This is also a border collision bifurcation (for the cycle on the boundary of the interval), and what occurs after a degenerate flip bifurcation is not known in general. A unique $2k$-cycle is left (which may be stable or unstable), or the dynamics may be chaotic (we shall see both occurrences in our model).

Let us start with the equilibrium of the map: the fixed point which comes from the function on the right side. From $f_R(x_R^*) = x_R^*$ we have the fixed point $x_R^* = \frac{m_R}{1-s_R} > 0$ which is attracting for $-1 < s_R < 0$. A degenerate flip bifurcation occurs when $s_R = -1$, which means that at the bifurcation value all the points of the absorbing interval I:

$$I = [f_R^2(0), f_R(0)] = [0, m_R], \tag{4}$$

are cycles of period 2 (except for the fixed point). After the bifurcation, only one cycle of period 2 may be left, or not. A 2-cycle must necessarily be of symbolic sequence LR, and the two periodic points can be easily found, solving for $f_L \circ f_R(x) = x$ which gives the periodic point on the R side, and solving for $f_R \circ f_L(x) = x$ which gives the periodic point on the L side, so that we obtain

$$x_0 = \frac{s_R m_L + m_R}{1 - s_L s_R} < 0, \quad x_1 = \frac{s_L m_R + m_L}{1 - s_L s_R} > 0. \tag{5}$$

The 2-cycle, when existing, is stable for $-1 < \lambda_2 = s_R s_L < 0$. Its existence is associated with the condition given by the numerator of x_0 (as the denominators are always positive). That is: $s_R < -\frac{m_R}{m_L}$ and the border collision bifurcation leading to its existence is $s_R = -\frac{m_R}{m_L}$, at which $x_0 = 0$, while the second possible border collision bifurcation, associated with $x_1 = 0$ can never occur, as under our assumptions on the parameters we always have $(s_L m_R + m_L) > 0$.

So we can immediately see that in the continuous case, when $m_L = m_R$, the BCB of the 2-cycle reduces to $s_R = -1$ and thus it corresponds to the degenerate flip bifurcation

of the fixed point x_R^*. While in the discontinuous case, when $m_L > m_R$ the BCB of the 2-cycle is associated with a value $-1 < s_R < 0$ to which there corresponds an attracting fixed point. This means that the region of existence of the 2-cycle is overlapping with the region of stability of the fixed point, and the overlapped region is a region of bistability. In fact, in our assumptions $0 < s_L < 1$, so that when the fixed point is stable also the 2-cycle is stable. Thus, keeping fixed the values of the parameters m_L and m_R, at the degenerate flip bifurcation of the fixed point a 2-cycle will be left, attracting if $-1 < \lambda_2 = s_R s_L < 0$ or repelling if $s_R s_L < -1$.

Differently, in the discontinuous case with $m_L < m_R$, the BCB of the 2-cycle is associated with a value $s_R = -\frac{m_R}{m_L} < -1$, so that when the degenerate flip bifurcation of the fixed point occurs (at $s_R = -1$), a 2-cycle cannot exist and, as we shall see, the system enters in a chaotic behavior.

As stated above, our results are valid in general, whichever are the values of the parameters, under the restriction given in (2). However, and in order to simplify the exposition, in our figures we use a fixed value $m_R = 2$ (but it can be any positive value), and $m_L = 3$, $m_L = 1$ or $m_L = 0.1$, which can be substituted with any value $m_L \geqslant m_R$, $x_R^* \leqslant m_L < m_R$ or $m_L < x_R^*$, respectively, obtaining qualitative figures and bifurcations as described in the following sections, where we shall analyze what kind of stable cycles occur in the model when the fixed point x_R^* is unstable.

Fig. 2(a) presents the generic structure of the two-dimensional bifurcation diagram in the slopes (s_R, s_L) for case (ii), $x_R^* \leqslant m_L < m_R$, and we can see that there are two typical scenarios. For small values of the slope s_R, a sequence of periodicity regions with increasing periods exists, related to k-cycles with $k \geqslant 1$, which will be described in Section 3 (of symbolic sequence $L^k R$, with period increment 1). In the enlargement (see Fig. 2(b)), between the periodicity region of the fixed point x_R^* and the periodicity region of the 2-cycle, there exists an infinite sequence of periodicity regions of stable $2p$-cycles, of even periods only, of period increment with increment 2 (of symbolic sequence LR^{2k+1}), described in Section 4. While when $m_L \geqslant m_R$ the region of the stable fixed point leads directly to the dynamics of the first kind, so that a stable 2-cycle is always created, and only stable cycles of type $L^k R$, with period increment 1, exist. The white region in Fig. 2 represents parameters at which chaotic dynamics occur.

Differently, in the regime (iii), with $0 < m_L \leqslant x_R^*$, the possible dynamics are shown in the bifurcation diagrams of Fig. 2(c) and its enlargement in Fig. 2(d). We can see that there is a region of period adding structure, below a stability curve (S) (that will be explained in Section 5). There is a family of regions of basic cycles, which in Fig. 2(d) is the family of regions associated with cycles of symbolic sequence $L^k R^2$ for any integer $k \geqslant 1$, and the adding rule

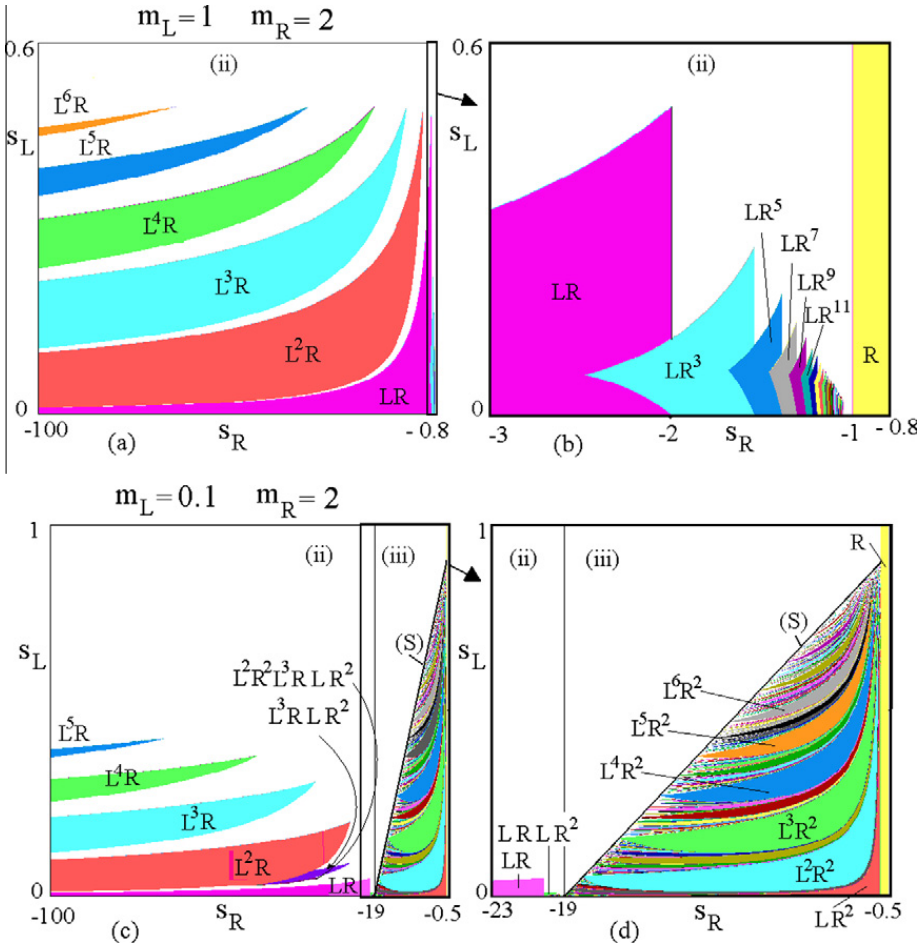

Fig. 2. Two-dimensional bifurcation diagram in the plane (s_R, s_L) at $m_L = 1$ and $m_R = 2$ in (a) and the enlarged portion in (b). $m_L = 0.1$ in (c) and the enlarged portion in (d).

works: between any two regions there are families of infinite regions associated with cycles with the symbolic sequence constructed as in the usual adding structure, as described in Section 5.

Another view of the periodicity regions existing in the three different cases is shown in Fig. 3 in the plane (s_R, m_L) at fixed values $s_L = 0.1$ and $m_R = 2$. In this figure we can see the three regions: (i) and (ii) separated by the line $m_L = m_R$, here $m_L = 2$, and (ii) and (iii) separated by the curve

$$m_L = x_R^*\left(= \frac{m_R}{1 - s_R}\right), \tag{6}$$

which corresponds, as remarked above, to the homoclinic bifurcation of the fixed point.

In the region (ii) we can see the periodicity tongues with overlapped portions leading to bistability, and described in Section 4, while in the region (iii) we can appreciate a period adding structure different from the one shown in Fig. 2(d), as described in Section 5, below the curve (S), boundary of the stability regime. We remark that no overlapped regions exist in case (iii).

The chaotic regime in this kind of maps is associated with *cyclical chaotic intervals*, and chaos is called *robust*(see [14]) because it is persistent with respect to parameter variations. Depending on the bifurcation structures occurring in the adjacent periodic domain, the chaotic region is organized by different bifurcation structures formed by contact bifurcations (or crises) as recently reported in [10]. Especially, close to the bifurcation structure described in Section 4, the chaotic domain is organized by the recently discovered bandcount incrementing structure, reported in [1–3]. By contrast, close to the period adding structure described in Section 5, the chaotic domain is organized by the self-similar bandcount adding structure introduced in [5,9]. We shall see some typical numerical examples for 1D bifurcation diagrams in the following sections. However, as already noticed, the different kinds of cyclical chaotic intervals occurring in the model are not investigated in this work. Here we are mainly interested in the regimes associated with the attracting cycles, whose periodicity regions are shown in Figs. 2 and 3.

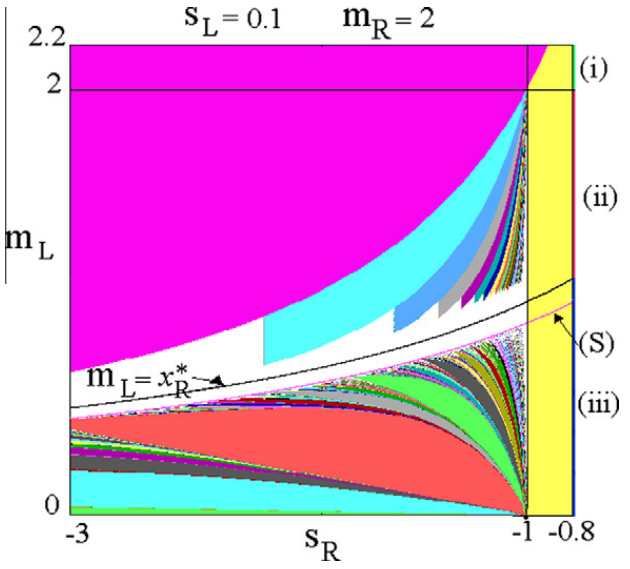

Fig. 3. Bifurcation diagram in the plane (s_R, m_L) at fixed values $s_L = 0.1$ and $m_R = 2$.

3. Maximal cycles L^kR

In this section we describe the BCB curves which are involved in the period increment scenario in which the period increases by one. As it is clear from Figs. 2 and 3, such periodicity regions are associated with periodic orbits having the symbolic sequence L^kR. To determine the border collision bifurcation curves we compute the periodic point of the $(k+1)$-cycle, in order to find at which parameter there is a collision with the discontinuity point $x = 0$, and to have its existence regions.

Thus let us call x_0 the point of the $(k+1)$-cycle which is immediately on the right of the discontinuity point $x = 0$. Then the periodic point $x_0$of the orbit of symbolic sequence L^kR can be obtained as the fixed point of the function $f_L^k \circ f_R(x)$, that is, solving for $f_L^k \circ f_R(x) = x$.[3] We have:

$$f_L^k \circ f_R(x) = s_L^k(s_R x + m_R) + m_L \frac{1 - s_L^k}{1 - s_L},$$

so that

$$x_0 = \frac{s_L^k}{1 - s_L^k s_R}\left[m_R + m_L \phi_k^L\right], \quad \phi_k^L = \frac{1 - s_L^k}{(1 - s_L)s_L^k} \tag{7}$$

and we notice that when the cycle exists, the denominator is always positive. The BCB leading to its existence occurs when the last periodic point of the cycle merges with the discontinuity point, $x_k = 0$, which also means $f_L(0) = x_0$ or $m_L = x_0$, that is: $\frac{1 - s_L^k s_R}{s_L^k} m_L = m_R + m_L \phi_k^L$, leading to the BCB curve given by the equation (for any $k \geqslant 1$):

$$BCB_{L^kR}: \; s_R = -\phi_{k-1}^L - \frac{m_R}{m_L}. \tag{8}$$

The curves bound the existence regions, given by $s_R < -\phi_{k-1}^L - \frac{m_R}{m_L}$, of these cycles of period $(k+1)$. We notice that this first BCB cannot be followed by a second one leading to the disappearance of the cycle, because, as we have seen for the cycle of period 2, for any such cycles we always have $x_0 > 0$, so that it can never merge with the boundary $x = 0$. It follows that it can only be attracting or repelling, before or after the degenerate flip bifurcation, which occurs when its eigenvalue $\lambda(L^kR) = s_L^k s_R$ crosses through -1. Thus the equation of the degenerate flip bifurcation curve of an existent $(k+1)$-cycle is given by $\lambda(L^kR) = s_L^k s_R = -1$, that is:

$$s_R = -1/s_L^k. \tag{9}$$

For $k = 1$ we get the points and the eigenvalue of the 2-cycle, and we note that the formulas given in (9) and in (8) also work for $k = 0$, giving the eigenvalue and the degenerate flip bifurcation of the fixed point x_R^* in the R side.

For increasing values of k, up to 6, the BCB curves given in (8) are drawn in black in Fig. 4(b), while the degenerate flip bifurcation curves given in (9) are drawn in red (grey).

[3] Clearly the 2-cycle is re-obtained for $k = 1$.

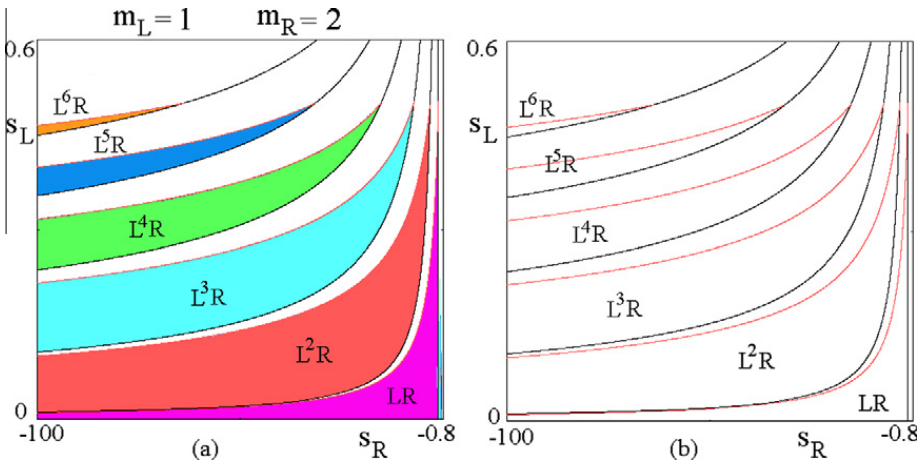

Fig. 4. Numerical (a) and analytical (b) BCB curves of the maximal cycles L^kR.

Moreover, we have an intersection point for each degenerate flip bifurcation curve with the BCB curve associated with the appearance of the cycle, determining for which values the cycle appears immediately unstable or stable (and a degenerate flip curve exists after that). The intersection point between the curves in (8) and in (9) satisfies the following condition:

$$\frac{1-s_L^{k-1}}{(1-s_L)s_L^{k-1}}-\frac{1}{s_L^k}+\frac{m_R}{m_L}=0,\quad s_R=-\frac{1}{s_L^k}, \tag{10}$$

giving the points on which the degenerate flip bifurcations curves start from the curves BCB_{L^kR}.

Fig. 5 illustrates a one-dimensional bifurcation diagram at $s_L = 0.3$ fixed, showing the dynamics of the state variable x as a function of the slope s_R. As we can see, decreasing s_R the degenerate flip bifurcations are always followed by cyclical chaotic intervals, which become a one-piece chaotic interval (after a short parameter interval).

We have described above the equations of the BCB leading to the appearance of cycles with symbolic sequence L^kR, and we have seen that a second BCB curve does not exist. This is the only possible dynamic behavior when $m_L \geqslant m_R$ and the fixed point is unstable, as the fate of the point $f_R(0) = m_R$ is the same as that of $f_L(0) = m_L \geqslant m_R$. So we notice that in such regimes it does not matter how is the definition of the map in the discontinuity point, $T(0) = m_R$ or $T(0) = m_L$, as both cases lead to the same attracting set, i.e. we get the same kind of dynamics.

This kind of dynamic behavior can exist also in case (ii), when $x_R^* \leqslant m_L < m_R$, for parameters in the left region with respect the 2-cycle, i.e. for $s_R \leqslant -\frac{m_R}{m_L}$ (as shown in Fig. 2(a)), while in the region (ii) with $s_R > -\frac{m_R}{m_L}$, as shown in the enlarged part of Fig. 2(b), we can have a different dynamic behavior, with periodicity regions which are overlapping, giving regions in the parameter space at which we have *two coexisting attracting cycles,* and the two different definitions of the map in the discontinuity point are values converging to two different cycles, as proved in the next section.

4. Maximal cycles LR^k

As stated above, the iterations may behave differently when $x_R^* \leqslant m_L < m_R$, and the fixed point is unstable, as in such a case the two points $f_L(0) = m_L$ and $f_R(0) = m_R$ may have a different dynamic behavior. This is not a new phenomenon. Indeed, when $x_R^* \leqslant m_L < m_R$ we can have not only cycles of the kind L^kR (when $s_R \leqslant -\frac{m_R}{m_L}$), but also cycles with symbolic sequence LR^k (when $s_R > -\frac{m_R}{m_L}$), and the reason is immediately clear looking at the graph in Fig. 1(b): when the value $f_L(0) = m_L$ is smaller than m_R and higher of x_R^*, we have that several applications of the function $f_R(x)$ in the R side are necessary before reaching the L side. Moreover, as we shall see below, the coexistence of two stable cycles of symbolic sequence LR^k and LR^{k+2} is allowed in suitable regions, for any odd integer $k \geqslant 1$.[4] In order to determine the existence regions of these new kind of cycles, let x_0 be the point of the cycle immediately on the left of the discontinuity point $x = 0$. Then the periodic point x_0 of the orbit with symbolic sequence LR^k can be obtained looking for the fixed point of the function $f_R^k \circ f_L(x)$, that is, solving for $f_R^k \circ f_L(x) = x$. The computations are similar to those already performed in the previous section, so that we obtain the same expression as given in (7) with R and L exchanged:

$$x_0=\frac{s_R^k}{1-s_R^k s_L}\left[m_L+m_R\phi_k^R\right],\quad \phi_k^R=\frac{1-s_R^k}{(1-s_R)s_R^k}$$

and setting $x_0 = 0$ we get the BCB curve of equation:

$$BCB_{LR^k}^{l}:\ m_L+m_R\phi_k^R=0, \tag{11}$$

denoted as $BCB_{LR^k}^{l}$. The upper index l indicates that at the border collision the periodic point x_0 of the cycle collides with the discontinuity point $x = 0$ from the left side. In

[4] As already noticed in [6], and as we shall describe later, the reason why the change in the period occurs by two units is due to the number of steps required for a point on the right side to reach the left one, which necessarily changes by two units, due to the swirl around the unstable fixed point.

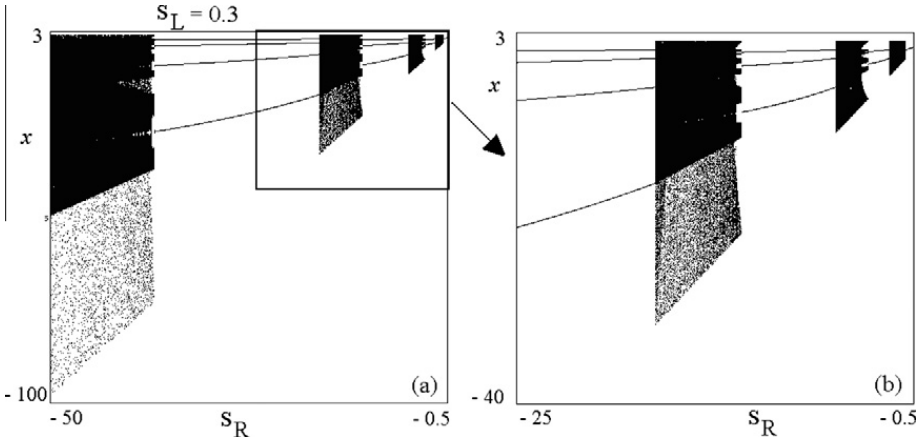

Fig. 5. One-dimensional bifurcation diagram in (a) with an enlargement in (b).

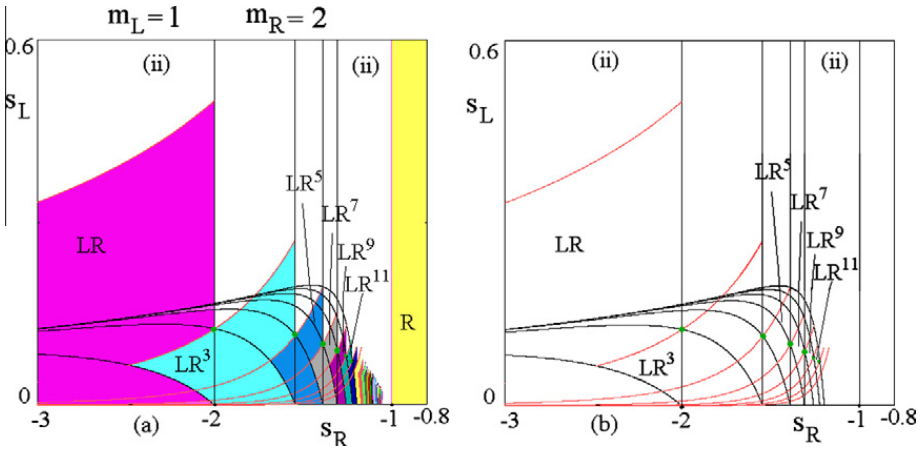

Fig. 6. Numerical (a) and analytical (b) BCB curves of some maximal cycles LR^k. The $BCB^l_{LR^k}$ are the vertical lines, while the other black curves denote the $BCB^r_{LR^k}$. The flip bifurcation curves are drawn in red (grey). (For interpretation of the references to colour in this figure legend, the reader is referred to the web version of this article.)

the parameter plane (s_R, s_L) such curves are vertical lines $s_R = const.$ where the constant value is determined by the equations in (11). A few of such lines are shown in Fig. 6.

We notice also that the cycle undergoing a BCB at the curve $BCB^l_{LR^k}$ has a periodic point $x_1 = f_L(x_0) > x^*_R$. In fact, by assumption at the bifurcation value we have $f_L(0) = m_L \geqslant x^*_R$ and thus the existent cycle starts with a periodic point $x_1 = f_L(x_0) > x^*_R$, which implies that the periodic point x_1 may be mapped in the L side after necessarily an even number of applications of the function $f_R(x)$, so that *such cycles exist only when k is an odd number,* and the period $(k+1)$ *even.*

Moreover, it is plain that such cycles exist only as long as another border collision bifurcation occurs, due to the periodic point x_{k-1} (*which implies* $k > 1$) merging with the discontinuity point $x = 0$. Equivalently, the cycle exists as long as the periodic point x_k merges with the maximum value $f_R(0) = m_R$. That is to say, $x_{k-1} = 0$ iff $x_k = m_R$ iff $x_0 = f_R(m_R)$. We have thus the second BCB curve, obtained by the equation $x_0 = m_R(1 + s_R)$, that is:

$$\frac{s_R^k}{1 - s_R^k s_L}\left[m_L + m_R \phi_k^R\right] = m_R(1 + s_R), \tag{12}$$

which leads to:

$$BCB^r_{LR^k}: \; s_L = \frac{1}{s_R^k} - \frac{m_L}{m_R(1 + s_R)} - \frac{\phi_k^R}{(1 + s_R)}, \tag{13}$$

denoted $BCB^r_{LR^k}$ because at the border collision the periodic point x_{k-1} of the cycle collides with the discontinuity point $x = 0$ from the right side. A few BCB curves of both sides, from (11) and (13), are shown in black in Fig. 6. We have noticed above that such bifurcation curves $BCB^r_{LR^k}$ exist only for $k > 1$, as for $k = 1$ we have the 2-cycle, already commented in Section 2.

From Fig. 6(a) we can see that the cycles here determined may be stable or unstable. The stability is associated with the related eigenvalue, which we know must be negative, because we have an odd number of periodic points in the R region, so that:

$$\lambda(LR^k) = s_L s_R^k < 0 \tag{14}$$

and its degenerate flip bifurcation occurs at $\lambda(LR^k) = s_L s_R^k = -1$, that is

$$s_L = -1/s_R^k. \tag{15}$$

The related degenerate flip bifurcation curves are drown in red in Fig. 6.

The green points in Fig. 6 also emphasizes that the calculated degenerate flip bifurcation curves always intersect in the same point two BCB curves. That is: *each curve* $BCB^{l}_{LR^k}$ *and* $BCB^{r}_{LR^{k+4}}$ *are intersecting in a point belonging to the degenerate flip bifurcation curve of the cycle* LR^{k+2}, *which proves that at most two stable cycles can coexist*. This property can be easily verified from the related equations. In fact, by using the relation

$$\phi^R_{k+1} = \phi^R_k + \frac{1}{s_R^{k+1}}, \tag{16}$$

after some algebra, substituting $\phi^R_k = -\frac{m_L}{m_R}$ from (11) and $s^k_R = -\frac{1}{s_L s_R^2}$ from (15) for the cycle LR^{k+2}, it follows that the equation of $BCB^{r}_{LR^{k+4}}$ (from (13)) is identically satisfied.

The relevant result in this regime is that a stable cycle may be not the only existent cycle, i.e. may be not globally attracting, as we have seen that we can have a stable cycle and also several unstable cycles placed on the basin boundary of the stable one. Moreover, in particular overlapping stability regions we have *coexistence of two stable cycles*.

Two different one-dimensional scenarios are shown in Fig. 7, for the state variable x as a function of the slope s_R (at two different values of s_L). In Fig. 7(a) we can see periodicity regions for stable cycles separated by regions with cyclical chaotic intervals, while in Fig. 7(b) we can see sequences of stable cycles only, and clearly we have coexistence in small intervals between two different cycles of even period k and $k+2$. We notice that this regime denoted by (ii) can include also different stability regions, and also overlapping regions, associated with different *period increment rules*.

As we can see in Fig. 2(d), below the stability region of the 3-cycle L^2R there are other stability regions, overlapping in pair, as well as on the right side of the stability region of the 2-cycle (as it will be better illustrated in the enlargement in Fig. 11 in the next section). The technique to determine the BCB curves is the same as the one used in this section, and the overlapping stability regions have the same properties. The main point is that in this region (ii) we cannot have the period adding structure, which exists in regime (iii), as described in the next section.

5. Period adding structure

Let us now consider the case (iii) $0 < m_L < x^*_R$, where a different and interesting dynamic behavior occurs, as it can be clearly seen from Fig. 2(d) and Fig. 3 below the curve $m_L = x^*_R$, that is, $m_L = \frac{m_R}{1-s_R}$. Let us first detect the periodic orbits from which the *period adding structure* shown in Fig. 2(d) can be started. By assumption we have now $m_L < x^*_R$ so that at the bifurcation value (of a point colliding with $x = 0$ from the left side) we have $f_L(0) = m_L < x^*_R$ and thus the existent cycle starts with a periodic point which must do at least two steps around the unstable fixed point before reaching the L side again. That is, such cycles have the symbolic sequence given by L^kR^2, for $k \geqslant 1$, and the cycle of least period (different from the fixed point) is a 3-cycle with symbolic sequence LR^2. Let us call x_0 the point of the cycle which is immediately on the left of the discontinuity point $x = 0$. Then the periodic point x_0 of the orbit of symbolic sequence L^kR^2 can be obtained as the fixed point of the function $f^{k-1}_L \circ f^2_R \circ f_L(x)$, that is, solving for $f^{k-1}_L \circ f^2_R \circ f_L(x) = x$. From:

$$f_L(x) = s_L x + m_L,$$
$$f^2_R \circ f_L(x) = s^2_R s_L x + s^2_R m_L + s_R m_R + m_R,$$
$$f^{k-1}_L \circ f^2_R \circ f_L(x) = s^{k-1}_L [s^2_R s_L x + s^2_R m_L + s_R m_R + m_R] + m_L \frac{1 - s^{k-1}_L}{1 - s_L},$$

we have

$$x_0 = \frac{s^{k-1}_L}{1 - s^k_L s^2_R} \left[s^2_R m_L + s_R m_R + m_R + m_L \phi^L_{k-1} \right], \tag{17}$$

where ϕ^L_k is defined in (7), and setting $x_0 = 0$ we have the BCB curve:

$$BCB^{l}_{L^kR^2} : \; s_R = \frac{1}{2m_L} \left[-m_R \pm \sqrt{m^2_R - 4m_L(m_R + m_L \phi^L_{k-1})} \right]. \tag{18}$$

Both the branches, due to the ± components, are used to draw the BCB curves in Fig. 8(b), determining the lower

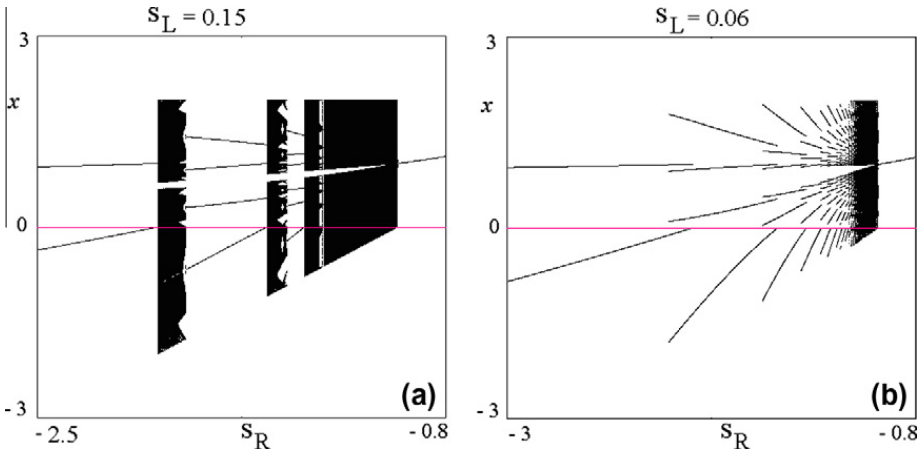

Fig. 7. One-dimensional bifurcation diagrams.

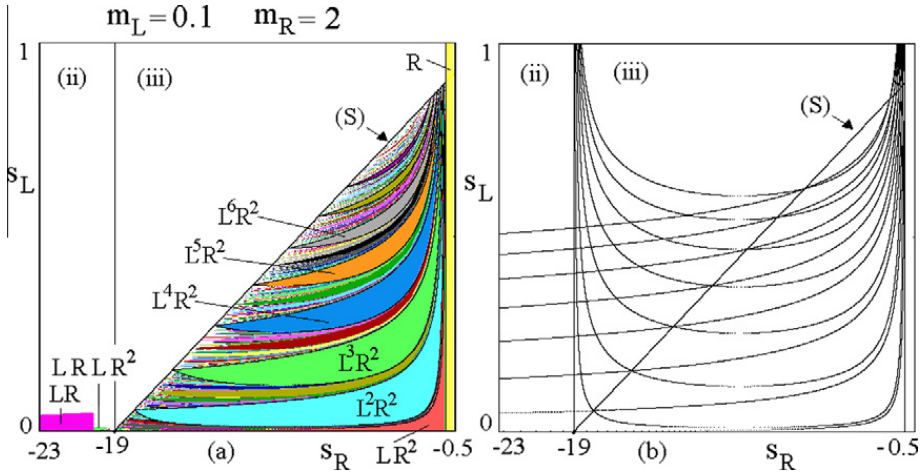

Fig. 8. Numerical (a) and analytical (b) BCB curves of cycles characterized by the symbolic sequence L^kR^2. For the lower boundaries given in (19), the portions with + (resp. −) are on the right (resp. left) of the point $s_R = -\frac{m_R}{2m_L}$ here equal to −10.

boundary of the periodicity regions shown in the stable regime (the right side with respect to the set (S) which will be described below), and the upper boundary in the unstable region (on the left side of the locus (S)).

Then such a cycle exists as long as the periodic point x_0, the first periodic point on the left side of the discontinuity point $x = 0$, merges with the preimage of the origin on the left side, i.e. the point $x^L_{-1} = f_L^{-1}(0) = -\frac{m_L}{s_L}$ (or, equivalently, as long as the periodic point of the cycle closest to 0 from the right side merges with the discontinuity $x = 0$). So that the other BCB curves, causing the disappearance of the cycles, are obtained by the following equation $x_0 = -\frac{m_L}{s_L}$, that is:

$$\frac{s_L^{k-1}}{1 - s_L^k s_R^2}\left[s_R^2 m_L + s_R m_R + m_R + m_L \phi^L_{k-1}\right] = -\frac{m_L}{s_L},$$

which leads to the following BCB curves:

$$BCB^r_{L^kR^2}: \; s_R = -1 - \frac{m_L}{m_R s_L^k} - \frac{m_L}{m_R}\phi^L_{k-1}, \tag{19}$$

a few of which (for $k = 1,\ldots,8$) are drown in Fig. 8, bounding the regions for the existence of the cycles L^kR^2.

The periodicity regions in which stable cycles L^kR^2 exist are disjoint, and it is expected the existence of cycles with different periods in between. Here the Farey sequence works. Let us remark that in the description of the periodicity regions we can associate a *rotation number* to each region, in order to classify all the periods and several cycles with the same period. In this notation a periodic orbit of period k is characterized not only by the period but also by the number of points in the two branches separated by the discontinuity point $x = 0$, already denoted by L and R, respectively. We can say that a cycle has a rotation number $\frac{q}{k}$ if a k-cycle has q points on the R side and the others $(k - q)$ on the L side. Then, between any pair of periodicity regions associated with the rotation numbers $\frac{q_1}{k_1}$ and $\frac{q_2}{k_2}$ there exists also the periodicity region associated with the rotation number $\frac{q_1}{k_1} \oplus \frac{q_2}{k_2} = \frac{q_1+q_2}{k_1+k_2}$ where $\oplus$ stands for the so-called Farey composition rule, or summation rule (see for example in [11]).

By extending a technique already proposed in [24,25,29] (see also [30] pp. 56–61 and pp. 80–84), we can call *regions of first level of complexity* those associated with the basic cycles L^kR^2 for $k \geqslant 1$. Then between any pair of consecutive *regions of first level of complexity*, say with rotation numbers $\frac{2}{k_1}$ and $\frac{2}{k_1+1}$, we can construct *two infinite families* of periodicity regions, called *regions of second level of complexity* via the sequence obtained by adding with the Farey composition rule $\oplus$ iteratively the first one or the second one, i.e. $\frac{2}{k_1+1} \oplus \frac{2}{k_1} = \frac{4}{2k_1+1}$, $\frac{4}{2k_1+1} \oplus \frac{2}{k_1} = \frac{6}{3k_1+1}$, $\frac{6}{3k_1+1} \oplus \frac{2}{k_1} = \frac{8}{4k_1+1}, \ldots$ and so on, that is:

$$\frac{2q}{qk_1+1} \text{ for any } q > 1 \tag{20}$$

and $\frac{2}{k_1} \oplus \frac{2}{k_1+1} = \frac{4}{2k_1+1}, \frac{4}{2k_1+1} \oplus \frac{2}{k_1+1} = \frac{6}{3k_1+2}, \frac{6}{3k_1+2} \oplus \frac{2}{k_1+1} = \frac{8}{4k_1+3} \ldots$, that is:

$$\frac{2q}{qk_1+q-1} \text{ for any } q > 1, \tag{21}$$

which give two sequences of regions accumulating on the boundaries of the two starting ones.

As the stable periodicity regions so obtained are disjoint, this mechanisms can be repeated: between any pair of contiguous "*regions of second level of complexity*", for example $\frac{2q}{qk_1+1}$ and $\frac{2(q+1)}{(q+1)k_1+1}$, we can construct two infinite families of periodicity regions, called "*regions of third level of complexity*" via the sequence obtained by adding with the composition rule $\oplus$ iteratively the first one or the second one and so on. All the infinitely many possible rational numbers are obtained in this way, giving all the infinitely many periodicity regions.

The Leonov technique, which has been improved in [21], can be used also in our context here, to get an iterative map in the coefficients, which leads to the analytical equations also of the border collision bifurcation curves of second complexity level and of further levels. To show the application of the process *it is enough to notice that locally we are in the same situation*. If we consider a parameter point which is between two consecutive periodicity regions of cycles of periods L^kR^2 and $L^{k+1}R^2$, in a neighborhood of the origin we have that the graph of the function

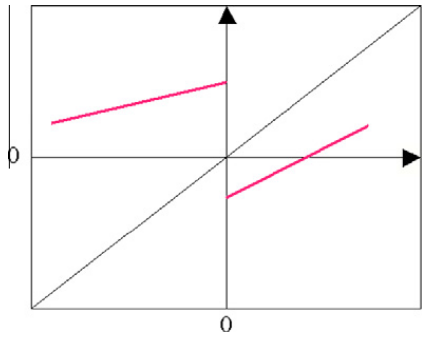

Fig. 9. The standard situation for applying the Leonov technique, occurring with the graph of the function $F_L(x) = f_L^k \circ f_R^2 \circ f_L(x)$ for $x < 0$ and the graph of the function $F_R(x) = f_L^k \circ f_R^2(x)$ for $x > 0$.

$F_L(x) = f_L^k \circ f_R^2 \circ f_L(x)$ for $x < 0$ and the graph of the function $F_R(x) = f_L^k \circ f_R^2(x)$ for $x > 0$ is that shown in Fig. 9, which is the standard situation in which the adding structure works. Thus considering the map $F(x)$ so defined, we can apply the iterative process described in [21].

That is, consider *the operator for the coefficients* defined by

$$x' = F(x) = \begin{cases} F_L(x) = A_L x + M_L & \text{if } x < 0, \\ F_R(x) = A_R x + M_R & \text{if } x > 0, \end{cases} \tag{22}$$

where to determine the BCB curves of the second level, we consider $F_L(x) = f_L^k \circ f_R^2 \circ f_L(x)$ and $F_R(x) = f_L^k \circ f_R^2(x)$, so that we have

$$\begin{aligned} &A_L = s_L^{k+1} s_R^2 \qquad (23)\\ &A_L = s_L^k s_R^2, \\ &M_L = s_L^k [s_R^2 m_L + s_R m_R + m_R + m_L \phi_{k-1}^L + m_L \phi_k^L], \\ &M_R = s_L^k [s_R m_R + m_R + m_L \phi_{k-1}^L + m_L \phi_k^L]. \end{aligned}$$

Then we obtain one family of the second complexity level by considering the functions $T(x) = F_R^n \circ F_L(x) = A_R^n A_L x + M_L A_R^n + M_R \frac{1-A_R^n}{1-A_R}$ for $n \geqslant 1$. We obtain the periodic point x^* of $T(x)$ (of the cycle with symbolic sequence $(L^k R^2)^n L^{k+1} R^2$) which is the first on the left of the origin, as follows:

$$M_R \leqslant x^* = \frac{1}{1 - A_R^n A_L} [M_L A_R^n + M_R \frac{1 - A_R^n}{1 - A_R}] \leqslant 0 \tag{24}$$

and we have the BCB curves via the equations $M_R = x^*$ and $x^* = 0$.

The second family is obtained similarly, by considering the functions $T(x) = F_L^n \circ F_R(x) = A_L^n A_R x + M_R A_L^n + M_L \frac{1-A_L^n}{1-A_L}$ for $n \geqslant 1$, the periodic point x^* of $T(x)$(of the cycle with symbolic sequence $(L^{k+1} R^2)^n L^k R^2$) which is the first on the right of the origin, is given by:

$$M_L \geqslant x^* = \frac{1}{1 - A_L^n A_R} \left[M_R A_L^n + M_L \frac{1 - A_L^n}{1 - A_L} \right] \geqslant 0 \tag{25}$$

and we have the BCB curves via the equations $M_L = x^*$ and $x^* = 0$.

The two families of the second level can be seen in the enlargement of Fig. 10 for $k = 2$, the first one accumulating on the periodicity region of the cycle $L^k R^2$ and the second family accumulating on $L^{k+1} R^2$. And so on, iteratively. Between any two pair of consecutive regions, we can construct in a similar way two infinite sequences of periodicity regions.

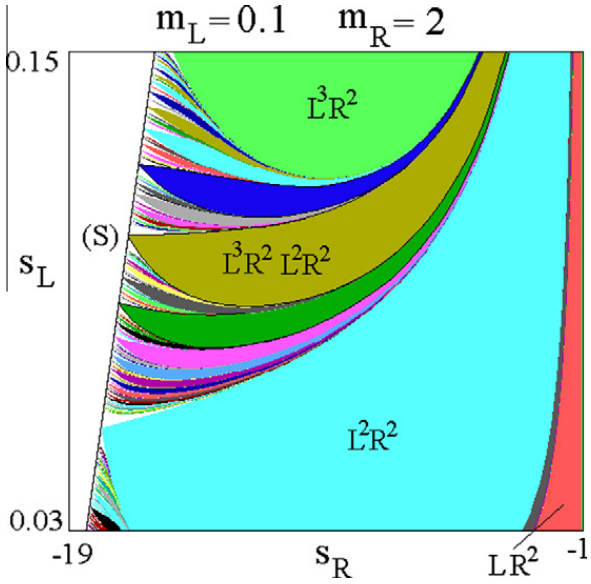

Fig. 10. BCB curves of the second and higher complexity level.

From Figs. 8 and 10 we can see that all the BCB curves bounding the stable cycles (of first complexity level $L^k R^2$ as well as all those of higher complexity level) intersect each other on a straight line of equation

$$(S): \; m_L(1 - s_R) - m_R(1 - s_L) = 0, \tag{26}$$

which is the locus in which the eigenvalues of all the cycles become equal to 1. To prove this statement we follow the arguments already used in [21] for the map with positive slopes.

Let us consider first the intersection point of the BCB curves of equations given in (18) and (19), bounding the existence region of the cycle $L^k R^2$ (whose eigenvalue is given by $\lambda = s_L^k s_R^2$). Parameters which satisfy (18) are such that (from (17)):

$$\begin{aligned} &s_R^2 m_L + s_R m_R + m_R + m_L \phi_{k-1}^L = 0, \\ &s_R^2 m_L + s_R m_R = -m_R - m_L \phi_{k-1}^L, \\ &s_R^2 \frac{m_L}{m_R} + s_R = -1 - \frac{m_L}{m_R} \phi_{k-1}^L \end{aligned}$$

and substituting into (19) we obtain:

$$\begin{aligned} &s_R - 1 - \frac{m_L}{m_R s_L^k} - \frac{m_L}{m_R} \phi_{k-1}^L, \\ &s_R = -\frac{m_L}{m_R s_L^k} + s_R^2 \frac{m_L}{m_R} + s_R, \\ &s_L^k s_R^2 = 1. \end{aligned}$$

This proves that on the locus (S) the cycles of first level of complexity have all the eigenvalue equal to 1. To prove that also all the infinitely many cycles constructed from them by the composition rule have eigenvalue equal to 1 it is enough to prove that for the BCB curves detected by

using the Leonov mechanisms shown above, on the locus (S) the following relation is also satisfied:

$$M_L(1-A_R)-M_R(1-S_L)=0, \tag{27}$$

from which it follows that the cycles related with the functions $T(x)=F_R^n\circ F_L(x)$ and $T(x)=F_L^n\circ F_R(x)$ have eigenvalue 1.

We notice that although we see periodicity regions filling the portion on the right side of the set (S) up to the stability region of the fixed point, the region is not filled by the existence of periodic orbits or the BCB curves. Some points in between are left, the complementary set, which is a set of zero Lebesque measure, and to such values of the parameters there correspond quasiperiodic trajectories (not chaotic, as no Cantor set of points can here exist). Also for the parameter points on the set (S): at a point of intersection of two BCB curves the map is conjugated with a linear rotation with rational rotation number (all the points are periodic with the same period), for the residual set of parameter values the map is conjugated with a linear rotation with irrational rotation number.

So the set (S) denotes the change of stability of all the cycles on the right side of the set: they also exist on the left side, but are unstable. For example, the existence region of the unstable cycles of first complexity level is between the curves with the same equations given in (18) and (19), but on the left side of (S).

Up to now we have described the region of adding structure existing above the stability region of the 3-cycle LR^2. However the adding structure exists also below the region of the 3-cycle LR^2. This can be seen in Fig. 11 which shows enlargements of the regions shown in Fig. 2(c) and (d) and of the leftmost corner of Fig. 8. In Fig. 11(b) the regions of first complexity level are those with symbolic sequence $(LR^2)^kR^2$.

In Fig. 11 we can also see that region (ii) includes a different family of bistability regions following the period increment scheme with increment of three (via LR^2).

We have already recalled that the existence of the set (S) and its role has been described also in [21], associated with the same map, but in a regime with positive slopes only, in which the adding structure applies to the periodicity regions of principal (or maximal) cycles, and in that case it was a separator between region with only stable cycles or quasiperiodic orbits or only chaos. Here also we have the same property: in case (iii) either we are below the locus (S) in a regular regime, or we are in the region between the locus (S) and the curve of equation $m_L=x_R^*$ in which chaos exists, and no stable overlapping regions can be found.

In Fig. 12 we show that region (iii) includes several kinds of adding structure. In fact, the periodicity regions of the adding structure in Fig. 12 can be obtained starting

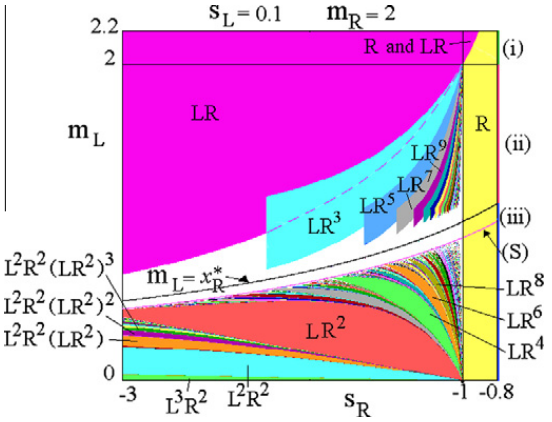

Fig. 12. Two dimensional bifurcation diagram in the plane (s_R, m_L).

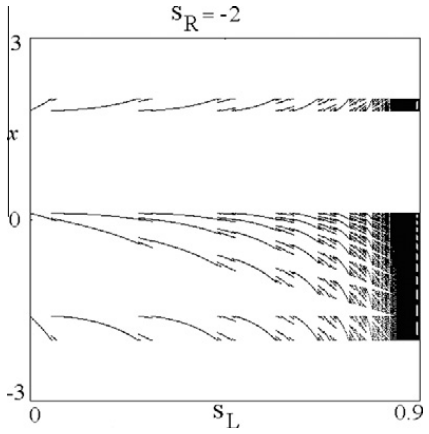

Fig. 13. One-dimensional bifurcation diagram at $m_L=0.1$, $m_R=2$, $s_R=-2$, showing the region of period adding structure.

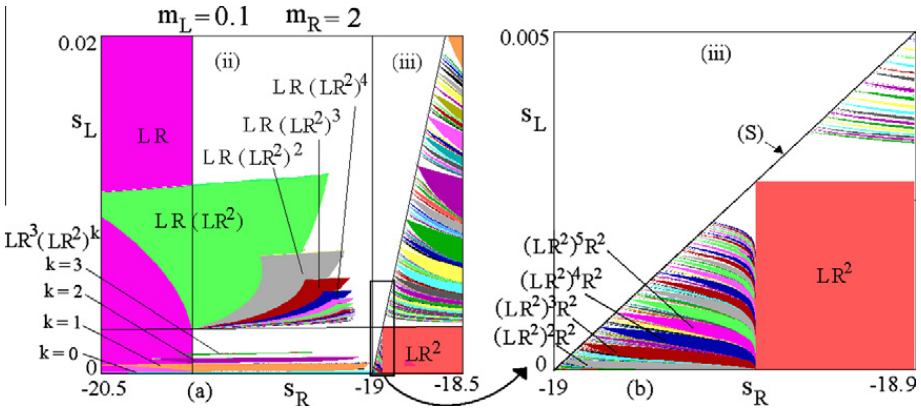

Fig. 11. Enlarged portions of two-dimensional bifurcation diagrams.

from the family of first level of complexity of symbol sequence LR^{2k}, for $k \geqslant 1$, and the mechanisms to detect the BCB bounding the periodicity regions is similar to the one described above.

We close this section showing in Fig. 13 a path in the region of stable cycles, where the structure associated with the period adding can be appreciated in the state variable x as a function of the parameter s_L at fixed $s_R = -2$.

6. Conclusions

In this work we have considered the generic piecewise linear discontinuous map with one stable increasing branch in the L side and a decreasing branch in the R side and positive offsets. We have determined the border collision bifurcation curves leading to the existence of stable cycles in three qualitatively different regimes for the values of the jump. In the case called (i), for $m_L \geqslant m_R$, only stable cycles of symbolic sequence L^kR can exist, whose BCB curves are given in Section 3. In the case (ii), for $x_R^* \leqslant m_L < m_R$ there are all the stable cycles LR^k for $s_R \leqslant -\frac{m_R}{m_L}$, while in the region $-\frac{m_R}{m_L} < s_R < -1$ there are overlapping periodicity regions for stable cycle of even periods only, of period increment type, whose BCB curves have been determined in Section 4, as well as other overlapping regions, always following the period increment rule. In the third case (iii), $0 < m_L < x_R^* (< m_R)$ we have detected, in Section 5, stability regions of period adding structure, starting from the cycles of first complexity level with symbolic sequence L^kR^2 and other families also exist. Still some regions are not explored, and some parameter constellations, for the models here considered, are left for further studies.

References

[1] Avrutin V, Eckstein B, Schanz M. The bandcount increment scenario. I. Basic Structures. P Roy Soc A-Math Phy 2008;464:1867–83.
[2] Avrutin V, Eckstein B, Schanz M. The bandcount increment scenario. II. Interior Structures. P Roy Soc A-Math Phy 2008;464:2247–63.
[3] Avrutin V, Eckstein B, Schanz M. The bandcount increment scenario. III. Deformed Structures, P Roy Soc A-Math Phy 2009;465:41–57.
[4] Avrutin V, Schanz M. On multi-parametric bifurcations in a scalar piecewise-linear map. Nonlinearity 2006;19:531–52.
[5] Avrutin V, Schanz M. On the fully developed bandcount adding scenario. Nonlinearity 2008;21:1077–103.
[6] Avrutin V, Schanz M, Banerjee S. Multi-parametric bifurcations in a piecewise-linear discontinuous map. Nonlinearity 2006;19: 1875–906.
[7] Avrutin V, Schanz M, Banerjee S. Codimension-3 bifurcations: Explanation of the complex 1-, 2- and 3d bifurcation structures in nonsmooth maps. Phys Rev E 2007;75:066205.
[8] Avrutin V, Schanz M, Gardini L. Calculation of bifurcation curves by map replacement. Int J Bifurcat Chaos, 2010;20:3105–35.
[9] Avrutin V, Schanz M, Gardini L. Self-similarity of the bandcount adding: calculation by map replacement. Regular and Chaotic Dynamics, 2010;15:683–701.
[10] Avrutin V, Schanz M, Schenke B. Coexistence of the bandcount-adding and bandcount-increment scenarios. Discrete Dynamics in Nature and Society 2011 (to appear).
[11] Bai-Lin H. Elementary Symbolic Dynamics and Chaos in Dissipative Systems. Singapore: World Scientific; 1989.
[12] Banerjee S, Karthik MS, Yuan GH, Yorke JA. Bifurcations in one-dimensional piecewise smooth maps – theory and applications in switching circuits. IEEE T Circuits-I 2000;47:389–94.
[13] Banerjee S, Verghese GC. Nonlinear Phenomena in Power Electronics: Attractors, Bifurcations, Chaos, and Nonlinear Control. New York: IEEE Press; 2001.
[14] Banerjee S, Yorke JA, Grebogi C. Robust chaos. Phys Rev Lett 1998;80:3049–52.
[15] Dankowicz H, Nordmark AB. On the origin and bifurcations of stick-slip oscillations. Physica D 2000;136:280–302.
[16] Day R. Irregular growth cycles. Am Econ Rev 1982;72:406–14.
[17] Day R. Complex Economic Dynamics. Cambridge: MIT Press; 1994.
[18] di Bernardo M, Budd CJ, Champneys AR, Kowalczyk P. Piecewise-smooth Dynamical Systems: Theory and Applications. Applied Mathematical Sciences 163. London: Springer-Verlag; 2007.
[19] di Bernardo M, Feigin MI, Hogan SJ, Homer ME. Local analysis of C-bifurcations in ndimensional piecewise smooth dynamical systems. Chaos Solitons Fractals 1999;10:1881–908.
[20] Foale S, Bishop SR. Bifurcations in impact oscillations. Nonlinear Dynam 1994;6:285–99.
[21] Gardini L, Tramontana F, Avrutin V, Schanz M. Border Collision Bifurcations in 1D PWL map and the Leonov approach. Int J Bifurcat Chaos 2010;20:3085–104.
[22] Halse C, Homer M, di Bernardo M. C-bifurcations and period-adding in one-dimensional piecewise-smooth maps. Chaos Solitons Fractals 2003;18:953–76.
[23] Ing J, Pavlovskaia E, Wiercigroch M, Banerjee S. Experimental study of impact oscillator with one-sided elastic constraint. Philos T Roy Soc A 2008;366:679–704.
[24] Leonov NN. On a map of a line into itself. Radiofisika 1959;2:942–56.
[25] Leonov NN. On a discontinuous map of a line into itself, Dokl. Acad. Nauk SSSR 1962;143:1038–41.
[26] Maistrenko YL, Maistrenko VL, Chua LO. Cycles of chaotic intervals in a time-delayed Chua's circuit. Int J Bifurcat Chaos 1993;3:1557–72.
[27] Maistrenko YL, Maistrenko VL, Vikul SI, Chua LO. Bifurcations of attracting cycles from time-delayed Chua's circuit. Int J Bifurcat Chaos 1995;5:653–71.
[28] Maistrenko YL, Maistrenko VL, Vikul SI. On period-adding sequences of attracting cycles in piecewise linear maps. Chaos Solitons Fractals 1998;9:67–75.
[29] Mira C. Sur les structure des bifurcations des diffeomorphisme du cercle. C.R.Acad Sc Paris Series A 1978;287:883–6.
[30] Mira C. Chaotic dynamics. Singapore: World Scientific; 1987.
[31] Nordmark AB. Non-periodic motion caused by grazing incidence in an impact oscillator. J Sound Vib 1991;145:279–97.
[32] Nusse HE, Yorke JA. Border-collision bifurcations including period two to period three for piecewise smooth systems. Physica D 1992;57:39–57.
[33] Nusse HE, Yorke JA. Border-collision bifurcation for piecewise smooth one-dimensional maps. Int J Bifurcat Chaos 1995;5: 189–207.
[34] Nusse HE, Ott E, Yorke JA. Border-collision bifurcations: An explanation for observed bifurcation phenomena. Phys Rev E 1994;49:1073–6.
[35] Puu T, Sushko I. Oligopoly Dynamics, Models and Tools. New York: Springer-Verlag; 2002.
[36] Puu T, Sushko I. Business Cycle Dynamics, Models and Tools. New York: Springer-Verlag; 2006.
[37] Sharan R, Banerjee S. Character of the map for switched dynamical systems for observations on the switching manifold. Phys Lett A 2008;372:4234–40.
[38] Sushko I, Gardini L. Degenerate Bifurcations and Border Collisions in Piecewise Smooth 1D and 2D Maps. Int J Bifurcat Chaos 2010;20:2045–70.
[39] Tramontana F, Gardini L, Dieci R, Westerhoff F. The emergence of 'Bull and Bear' dynamics in a nonlinear 3d model of interacting markets. Discrete Dyn Nat Soc 2009:310471.
[40] Tramontana F, Gardini L, Dieci R, Westerhoff F. Global bifurcations in a three dimensional financial model of "bull and bear" interactions. In: Chiarella C, Bischi GI, Gardini L, editors. Nonlinear Dynamics in Economics, Finance and Social Sciences. Berlin: Springer-Verlag; 2009.
[41] Tramontana F, Gardini L, Westerhoff F. On the complicated price dynamics of a simple one-dimensional discontinuous financial market model with heterogeneous interacting traders. J Econ Behav Organiz 2010;74:187–205.
[42] Zhusubaliyev ZT, Mosekilde E. Bifurcations and Chaos in Piecewise-Smooth Dynamical Systems. Singapore: World Scientific; 2003.